Accelerated Ray Tracing using R-Trees

Dirk Feldmann
Department Scene Analysis, Fraunhofer IOSB, Ettlingen, Germany

Keywords: Ray Tracing, R-Tree, Acceleration, Spatial Index, GPU, CUDA, Stackless Algorithm.

Abstract: Efficient ray tracing for rendering needs to minimize the number of redundant intersection tests between rays and geometric primitives. Hence, ray tracers usually employ spatial indexes to organize the scene to be rendered. The most popular ones for this purpose are currently kd-trees and bounding volume hierarchies, for they have been found to yield best performances and can be adapted to contemporary GPU architectures. These adaptations usually come along with costs for additional memory or preprocessing and comprise the employment of stackless traversal algorithms.
R-trees are height-balanced spatial indexes with a fixed maximum number of children per node and were designed to reduce access to secondary memory. Although these properties make them compelling for GPU ray tracing, they have not been used in this context so far.
In this article, we demonstrate how R-trees can accelerate ray tracing and their competitiveness for this task. Our method is based on two traversal schemes that exploit the regularity of R-trees and forgo preprocessing or alterations of the data structure, with the first algorithm being moreover stackless. We evaluate our approach in implementations for CPUs and GPUs and compare its performance to results we obtained by means of kd-trees.

1 INTRODUCTION

Efficient ray tracing needs to organize the objects of a scene in such a way that there are as few as possible redundant intersection tests between rays and the geometric primitives those objects consist of. This is usually accomplished by employing spatial indexes such as kd-trees, octrees, bounding volume hierarchies (BVHs) or various types of grids. Among these data structures, kd-trees and BVHs have received much attention in recent years, because they can be implemented on contemporary GPUs in order to harness their parallel computing capabilities.

R-trees (Guttman, 1984) were designed to index spatial data in large databases and aim for reducing access to secondary memory. They are height-balanced trees with arity usually > 2 and are used, for instance, in modern database management systems, like MySQL or Oracle Spatial (Oracle Corp., 2014a; Oracle Corp., 2014b). Their regularity makes R-trees well-suited for accelerating ray tracing, because it enables efficient stackless traversal schemes without additional costs for extra pointers or extensive preprocessing. Furthermore, the accompanying and potentially high memory locality of the contained data benefits the architectures of today's GPUs, whose performances are sensitive to cache misses. But to the best of our knowledge, R-trees have not yet been used as acceleration data structures in ray tracing.

In this work we describe how R-trees can be employed to accelerate ray tracing of static scenes and demonstrate their suitability for this task by means of a CPU-based ray tracer and a CUDA-based one. We present two different algorithms for ray traversal that exploit the regularity of R-trees: The first one is stackless, requires neither additional memory nor pointers and is superior to a conventional stack-based traversal scheme. Our second algorithm uses a small amount of additional memory and improves the performance of parallel ray tracing on GPUs in certain situations, compared to our stackless method. We furthermore compare the performance of our R-tree-based CPU implementation with results we obtain by means of kd-trees constructed using the popular surface area heuristic. The results indicate that R-trees can be competitive alternatives to kd-trees, but the traversal of R-trees is additionally more convenient than those of kd-trees or BVHs.

The remainder of this article is structured as follows: Section 2 summarizes the most important work related to ours and gives a description of R-trees, for these data structures appear to be less well known.

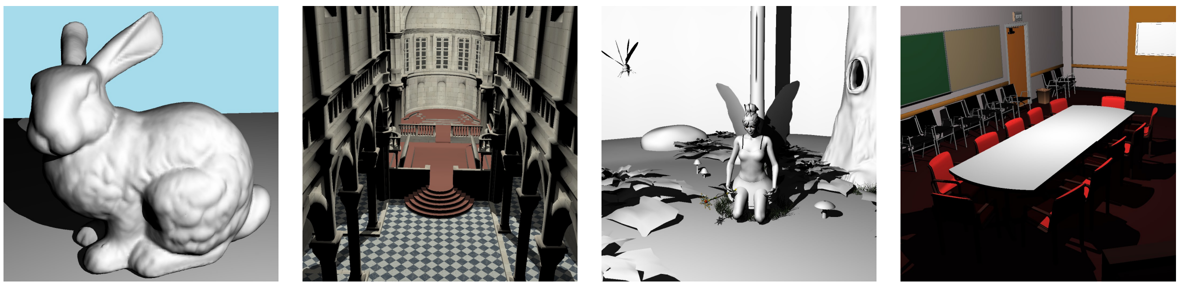

(a) `Bunny` (b) `Cathedral` (c) `Fairy` (d) `Conference`

Figure 1: We employed the depicted test scenes and camera poses to evaluate the methods presented throughout this work: (a) Standford Bunny, 69 632 triangles, (b) Sibenik Cathedral, 75 284 triangles, (c) a frame from the Utah Fairy Forest animation, 173 579 triangles, (d) Conference Room, 331 135 triangles.

SCITEPRESS SCIENCE AND TECHNOLOGY PUBLICATIONS

In Section 3, we enter on aspects that need consideration in order to use R-trees for accelerating ray tracing. The two different algorithms for determining intersections between rays and the geometric primitives indexed by R-trees are presented in Section 4. In Section 5, we evaluate the performance of our approach and discuss the results. Additionally, we compare the performance of our R-tree-based method for CPU ray tracing to results we obtain when using kd-trees instead. We conclude our work with a discussion and prospects of future research in Section 6. The test scenes we employed throughout this work are shown in Figure 1.

2 BACKGROUND AND RELATED WORK

By employing appropriate spatial indexes to keep the number of redundant intersection tests of rays with objects within a scene as small as possible, ray tracing implementations on modern GPUs can achieve interactive frame rates and beyond for *static* scenes (Horn et al., 2007). From the wide field of spatial indexes, which is covered in detail in (Samet, 2006), popular choices for organizing scenes have been various kinds of grids, octrees, kd-trees, general BSP-trees and bounding volume hierarchies (BVHs) (Suffern, 2007, p. 443). In the context of GPU ray tracing, many researchers found kd-trees and BVHs to be the most appropriate spatial indexes, because they yield good performances (Wächter and Keller, 2006; Stich et al., 2009) and can be adapted to processor architectures of GPUs (Hachisuka, 2009; Hapala et al., 2011; Hapala and Havran, 2011). The main difference between these two data structures is that BVHs partition scenes with respect to the objects, whereas kd-trees partition the underlying space.

R-trees (see Section 2.2) are spatial indexes that share properties with BVHs as well as with kd-trees, but have unique features of their own: Like BVHs, R-trees organize objects based on their minimal axis-aligned bounding boxes, but like in kd-trees, nodes are split with respect to locations in space determined by some heuristic (see Section 2.2.1). The resulting splits, however, are not necessarily strictly binary partitions of the underlying space, but rather resemble divisions in BVHs. In contrast to the latter ones, R-trees are balanced in height and are designed analogously to B-trees for reducing accesses to secondary memory by increasing the locality of data in memory. Furthermore, R-trees can be either constructed incrementally by successive insertion of data or by using methods for *bulk loading* all data at once (see (Sellis et al., 1987; Arge et al., 2008), for instance).

Although the features of R-trees indicate a good suitability for their application in ray tracing, which has been pointed out in (Sylvan, 2010), these data structures apparently have not been further examined in this context so far. Surprisingly, they are not even mentioned in recent surveys on ray tracing (Wald et al., 2007; Hachisuka, 2009) or articles on splitting BVHs (Stich et al., 2009).

2.1 KD-Trees and BVHs

Kd-trees have been reported to perform particularly well in ray tracing when being constructed by means of surface area heuristic (SAH) (MacDonald and Booth, 1990), but their most severe disadvantage has been for long time their high construction times. This limitation has been alleviated by algorithms for more efficient construction (Wald and Havran, 2006). Although the overall performance of kd-trees is frequently superior to those of BVHs, because kd-trees adapt better to the complexity of scenes, BVHs are often preferred due to their simplicity (Wächter and Keller, 2006; Stich et al., 2009). Other studies indicate that BVHs perform better for tracing coherent rays, whereas kd-trees are superior in case of incoherent rays (Zlatuska and Havran, 2010).

When implementing kd-trees or BVHs on GPUs, it is necessary to account for certain aspects of the underlying processor architecture: The local memory available to a GPU thread is significantly less than to programs running on CPUs. This impairs or even prevents the allocation large amounts of local memory and thus the employment of traversal algorithms that rely on stacks or queues, for instance. Hence, various methods for stackless kd-tree and BVH traversal have been developed (Hapala et al., 2011; Hapala and Havran, 2011), but they require additional processing steps or extra storage for pointers or traversal states.

Furthermore, the performance of GPU kernels strongly depends on the locality of data in memory and the number of cache misses, because the latter will delay the execution of a large number of threads at once. Presenting data in a coherent way by means of cache-friendly data structures and access patterns is thus an important issue.

More details on the employment of kd-trees and BVHs in ray tracing can be found in (Wächter and Keller, 2006),(Hachisuka, 2009) and (Wald et al., 2007), for example, where the latter article focuses on ray tracing of dynamic scenes.

2.2 R-Trees

R-trees (Guttman, 1984) are height-balanced spatial indexes related to B-trees (Bayer and McCreight, 1972). Data are stored based on their n-dimensional minimal axis-aligned bounding boxes (AABBs), which serve as keys and are commonly used to support point-location and window queries (Samet, 2006). Like with B-trees, only the leaf nodes at the lowest level $l = 0$ hold actual data. The entries of intermediate nodes at levels $l > 0$ point to nodes at the next lower level $l - 1$. Except for the root located at the topmost level L, each node contains at least $m > 0$ (usually $m \geq 2$) and at most $M > m$ entries. The root may hold less than m entries, especially if the tree is empty, but cannot contain more than M entries. Each node maintains an n-dimensional AABB that encloses the bounding boxes of the entries contained in that node. The structure of a 2D R-tree is illustrated in Figure 2.

When data are inserted into an R-tree, leaf nodes may *overflow* if they had to contain more than M entries and hence must be *split* into two. The resulting extra leaf is inserted at the original leaf's parent, which in turn may overflow as well. This can trigger cascades of node splits up to the root. If the root has to be split, the tree *grows* by adding a new level $L+1$

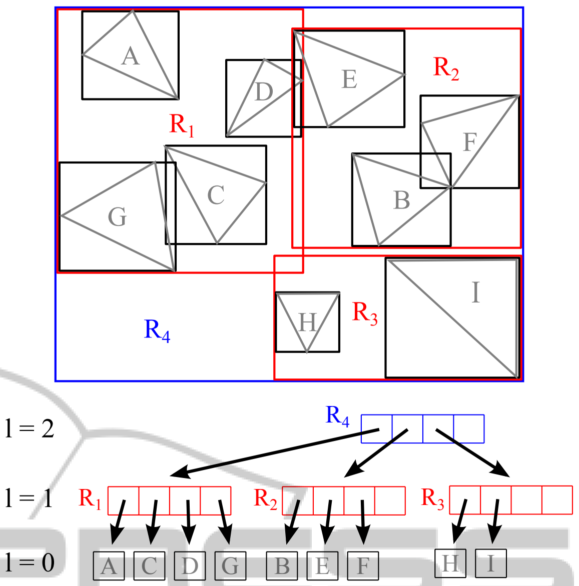

Figure 2: The data (triangles) A – I are stored in the leaf nodes of a 2D R-tree with $m = 2$ and $M = 4$ at level $l = 0$ based on their AABBs. Entries of nodes at levels $l > 0$ point to nodes at the next lower level. Each node maintains an AABB enclosing its entries (rectangles R_1 - R_4).

and a new root, which receives the former root and its new sibling become as the only children. Likewise, if data are removed, nodes may *underflow* and must hence be merged in order to satisfy the constraint of holding at least m entries. Whenever an entry is added or removed from a node, that node's AABB must be adjusted in such a way that it remains the minimal AABB for all of the node's entries. Except for the increased complexity that comes along with splitting nodes, the proceedings for adding data to or deleting data from R-trees is the same as with B-trees.

In order to split nodes, there are various strategies that directly influence the structure of an R-Tree and thus its performance in subsequent find operations. These strategies usually try to minimize properties of the AABBs of the resulting nodes, such as their volume, mutual overlap or surface, and are employed differently or mixed in R-Tree variants.

2.2.1 R-Tree Construction

As illustrated in Figure 2, objects and their AABBs stored in R-trees may overlap. Hence, the nodes, which we identify with their maintained AABBs, may also overlap each other at the same level. This impedes ray traversal, because all paths in the tree starting at locations where nodes overlap may lead to geometric primitives that may be intersected. In addition, nodes that include large amounts of *dead space*, i.e., space only occupied by AABBs, but not by actual geometric primitives, must be tested for intersections with rays, although the contained primitives may not be intersected at all. Therefore, it is desirable to avoid such situations by minimizing overlap and dead space during the construction of R-trees. Since optimizing for both these parameters at reasonable costs is infeasible in non-trivial situations, we have to rely on heuristics to yield well-structured R-trees.

In the following, we briefly present two existing approaches on building R-trees by successive insertion of data. At the level of leaf nodes, *data* are the geometric primitives to be stored in the R-tree. At the level of intermediate nodes, *data* are pointers to nodes at the next lower level. In any case, data must always be provided with their associated AABB.

For more details on the construction and split algorithms, we refer to the original articles (Guttman, 1984; Beckmann et al., 1990).

The approach for constructing R-trees in (Guttman, 1984) is formulated for AABBs in 2D and relies on selecting the node that requires the least area enlargement when data are inserted. Ties are resolved by selecting the node of least area. When nodes need to be split due to overflow, the entries are distributed in such a way that the total area occupied by the two resulting nodes (and thus dead space) is minimized.

The R^*-tree (Beckmann et al., 1990), a variant of the R-tree, uses different strategies for choosing nodes when inserting data at the levels of intermediate and leaf nodes. In the former case, entries (i.e., other nodes) are inserted at the node whose box needs least area enlargement; ties are resolved by selecting the node of least area. In case of leaf nodes, data are assigned to the node whose box will overlap least with those of its siblings afterwards; ties are resolved by using the node that requires least area enlargement.

Node splits in R^*-trees are performed by sorting the entries of a node according to the minimum and maximum values of their AABBs in each dimension d. For each of the $2d$ sorts, a series of partitions into two sets is constructed: The first i entries in the sort, where $m \leq i \leq M+1-m$, are assigned to the first set of the i-th partition and the remaining $M+1-i$ ones to the second set. Each of these partitions along one of the d axes represents a possible redistribution of the entries from the overflowing node into two nodes. The perimeters of all these candidates are summed up, and the overflowing node is split along the axis where the sum is minimal. Once the split axis has been determined, the entries are distributed according to the associated partition in which the two candidates have least area overlap.

In addition, the R^*-tree extends the original R-tree by using a technique called *forced reinsert*: As a node ν overflows, instead of immediately splitting it, its entries are sorted with respect to the distances of their boxes' centers from the center of ν's box. Depending on choice, the k entries with greatest or least distance are removed (*ejected*) from ν. Starting at the tree's root, the ejected entries are then tried to be reinserted at their respective levels. As a result, they may become assigned to different parents at the level of ν, because these new parents may have become better choices with respect to the tree's structure and the criterion for selecting nodes. In this way, the node occupancy is increased and potentially expensive split operations are delayed. If the ejected entries cannot be reinserted or if reinsertion would assign all of them again to their original parent, a split must be performed anyway.

In more recent work in (Beckmann and Seeger, 2009), the authors present the *revised R^*-tree (RR^*-tree)*. This variant employs modified strategies for splitting and selecting nodes that supersede the need for forced reinserts.

3 RAY TRACING USING R-TREES

For the purpose of ray tracing, spatial indexes are usually traversed to determine the object that is intersected by the ray at least distance from the origin of that ray. R-trees have similarities to BVHs, as they hold AABBs at every node, and ray traversal is analog: Starting at the root, the maintained box is checked for intersection with a given ray. If the ray intersects the box, each of the $n \in [m, M]$ children's boxes is tested for intersection with the ray, and the process is recursively repeated for each positively tested child node. In case the ray does not intersect a box, the entries contained within that node do not need to be considered any further, since they are not intersected the ray either. The process terminates as soon as all candidate objects at level $l = 0$ have been tested.

Due to their structure, R-trees have certain properties that make them particularly interesting for accelerating ray tracing: In contrast to common BVHs or kd-trees, R-trees are always balanced in height, i.e., all leaf nodes storing geometric primitives are located at the same level (*depth*). Hence, paths from the root towards leaves have constant lengths. Furthermore, the number of nodes per level is limited by the value chosen for M. This regularity allows to traverse R-trees without maintaining an auxiliary stack and to keep the memory consumption during traversal constant, which is of special importance for parallel ray tracing on GPUs, where the tree is traversed by multiple rays simultaneously.

3.1 Considerations for Ray Tracing

The equivalents of area and perimeter of 2D boxes in 3D are volume and surface, respectively, and overlap is the common volume occupied by two or more boxes. As pointed out in Section 2.2.1, the amounts of dead space and overlap between nodes influences the performance of R-trees. The amount of dead space depends on the quality of approximations of the geometric primitives by AABBs (and thus on the geometry of the scene), on the choice of data assignment to nodes and on the strategy for splitting nodes. The latter two aspects also influence the amount of mutual overlap.

Furthermore, R-tree nodes must be split if they exceed their limit of M entries, but the resulting nodes must not contain less than m entries. Since m and M determine how many entries must be checked if a ray intersects the containing node, these two parameters will influence the performance of R-trees as well.

Another aspect that influences ray tracing performance is the order in which the n child nodes (entries) are visited and is illustrated in Figure 3: Preferably, the entries of R-tree nodes are stored in a coherent block of memory, e.g., in an array, but visiting them in their order in memory is not necessarily optimal. Hence, the R-tree's ray tracing performance changes with the direction of rays. For the purpose of early ray termination, the best sequence for visiting entries would be the one obtained by sorting the contained geometric primitives according to their distances from a ray's origin in increasing order. This order, however, is usually not known in advance.

In summary, when using R-trees for ray tracing, their performance is influenced by the following factors:

- the underlying geometry of the scene
- the strategy for assigning entries to nodes
- the strategy for splitting nodes
- the number of entries per node, i.e., m and M
- the order in which children of nodes are tested for intersections with rays

4 RAY TRAVERSAL

Ray traversal in R-trees and its variants is similar to the proceeding employed with BVHs (see Section 3).

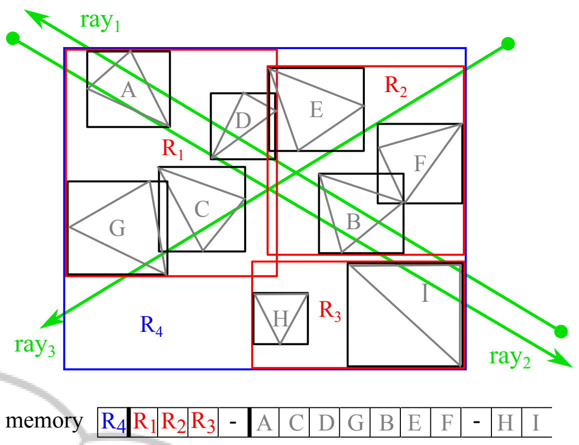

Figure 3: If the R-tree in Figure 2 is intersected by rays, the order in which nodes are tested for intersection influences the data structure's performance. In case of visiting nodes in the depicted memory order, the intersection at triangle I is closest to ray$_1$, but is found only after $R_1, A, C, D, G, R_2, B, E, F, R_3$ and H have been tested. The intersection at A is closest to ray$_2$ and is found first by chance. Thus, testing the entries of R_2 and R_3 is needless. ray$_3$ intersects C, but R_2 and its children need to be tested for intersection as well, because these boxes are closer to that ray's origin.

In contrast to most trees and BVHs, R-trees are balanced in height, which allows us to derive the following relations:
The total number of nodes N in an R-tree of height $L+1$ holding at most M entries per node is given by

$$N = \sum_{i=0}^{L} M^i = \frac{M^{L+1}-1}{M-1}$$

where $N, L, M \in \mathbb{N}$. Starting at the root, we may number all nodes in level order from left to right, including empty nodes (see Figure 4), and store the whole tree sequentially in an array.

Since there are M^{L-l} nodes at level $l \leq L$, the first node at l is located at position $\Delta_L(l)$ within the array, where

$$\Delta_L(l) = \begin{cases} 0 & l = L \\ \sum_{i=0}^{L-(l+1)} M^i & l < L \end{cases}$$

Given an intermediate node's index n and level $l > 0$, the index n_e of its first child/entry is

$$n_e = n_e(n) = (n - \Delta_L(l)) \cdot M + \Delta_L(l-1)$$

Likewise, if $l < L$, the index n_p of a node's parent is

$$n_p = n_p(n) = \left\lfloor \frac{(n - \Delta_L(l))}{M} \right\rfloor + \Delta_L(l+1)$$

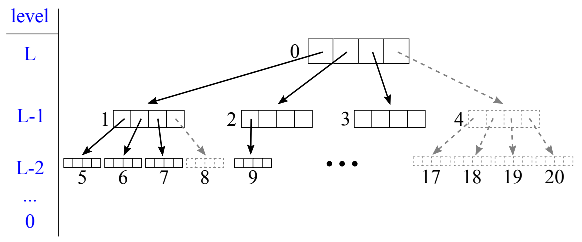

Figure 4: Level-order numbering of nodes in an R-tree with $M = 4$. Empty nodes (dashed gray line style) must be numbered as well. Nodes from levels below $L-2$ are omitted for the sake of clarity.

The position k, $0 \leq k < M$, of n within its parent n_p is computed by

$$k = \chi(n) = (n - \Delta_L(l)) \bmod M$$

Based on these relations, we devise the following two algorithms for traversing R-trees and computing the closest intersection of the contained geometric primitives with a given ray, if any such intersection exists. The algorithm presented in Section 4.1 is a straightforward implementation of depth-first traversal, but forgoes any additional stack. In Section 4.2, we present a second traversal scheme that visits nodes in the order of their distances from a ray's origin. Hereinafter, we assume that the primitives stored in the R-trees are triangles, for they are very common in rendering. A comparison of the performance of the two algorithms is presented in Section 5.2.

4.1 Stackless Ray Traversal

Our algorithm for stackless depth-first traversal of R-trees is given in the pseudo code in Listing 1.

If the given ray intersects a box or a triangle, function `intersects()` returns the distance t from that ray's origin to the location of its first intersection with the object. Otherwise, the function returns ∞. The result t_{min} of the algorithm is the minimum of all distances obtained from intersections of a given ray with triangles. If there are no intersections, $t_{min} = \infty$.

The loop starting at line 21 locates the next sibling of the current node n by examining whether n is the last entry within its parent, i.e., $\chi(n) = M - 1$. If so, the process is repeated for the parent of n until either an ancestor n' of n with $\chi(n') < M - 1$ has been found or the root node has been reached again. Otherwise, if $\chi(n) < M - 1$, n' is set to n. The algorithm then continues with the next node $n' + 1$. In this way, all relevant nodes will be visited, and the algorithm is guaranteed to terminate as soon as it has processed the last entry of the root.

```
1   $t_{min} = \infty$;
2   for ($n = 0, l = L$; $n < N$; ) {
3     proceedWithChild? = false;
4     if (! isEmptyNode($n$)) {
5       $t$ = intersects(ray, getBox($n$));
6       if (($t < \infty$) $\wedge$ ($t < t_{min}$)) {
7         if ($l > 0$) // visiting intermediate node
8           proceedWithChild? = true;
9         else { // visiting leaf node
10          foreach (triangle of $n$ as tri) {
11            $t_{tri}$ = intersects(ray, tri);
12            if (($t_{tri} < \infty$) $\wedge$ ($t_{tri} < t_{min}$))
13              $t_{min} = t_{tri}$;
14        } } } }
15    if (proceedWithChild?) {
16      $n = n_e(n)$; // proceed with first child...
17      $--l$; // ... at the next lower level
18    } else {
19      $n' = n$;
20      // If n is last entry within its
            parent,...
21      while (($l < L$) $\wedge$ ($\chi(n') == M - 1$)) {
            (*@\label{lbl:line-loop}@*)
22        $n' = n_p(n)$; // ...try parent of n...
23        $++l$; // ...at the next higher level
24      }
25      if ($l < L$)
26        $n = n' + 1$; // proceed with next sibling
27      else  // or, if still at the root,...
28        $n = N$; // ...exit loop at next iteration
29    }
30  }
31  return $t_{min}$;
```

Listing 1: Pseudo code for our algorithm for stackless ray traversal in R-trees. The syntax is borrowed from the programming languages C/C++.

4.2 Ordered Ray Traversal

The algorithm in Listing 1 suffers from the problem described in Section 3.1: Its performance depends on the directions of rays and on the order in which child entries are stored in memory. In case of primary rays, for instance, the effect becomes apparent by differences in frame rates as the virtual camera is placed at opposite locations of the scene, but looks at the same point. However, if the mutual overlap between nodes at the same level is low, there is a good chance that an AABB located closer to a ray's origin contains a geometric primitive that is also intersected by that ray at less distance than a primitive in an AABB further away.

Based on this consideration, we devised another algorithm for ray traversal in R-trees that relies on sorting node entries and requires a small amount of additional memory per ray: For each level l, we allocate a small stack and a pointer to its top and start ray traversal at the root of the R-tree. Each entry of

SCITEPRESS SCIENCE AND TECHNOLOGY PUBLICATIONS

a node at $l > 0$ that is intersected by a given ray is pushed onto the stack of level l. We then sort the entries on the stack according to the distances of their first intersection with that ray in decreasing order. The entry with least distance is thus located at the top of the stack, and the one with largest distance at the bottom. We repeat the process with the first node pointed to by the stack pointer at level l. Note that this node is located at $l-1$. If we arrive at a leaf, we test the contained triangles for intersection with the ray and update the overall minimal distance t_{min}, if necessary. If a node turns out to be empty or is missed by the ray, we proceed with the next node on the stack of level l. When a stack runs empty, we ascend in the tree by increasing the level and continue with nodes from the corresponding stack. The algorithm terminates as soon as the stack of the topmost level runs empty.

Since each stack has to hold at most M entries at a time, it can be implemented by an array of fixed size. Provided that the node entries and stack pointer are numbers of the same data type, the amount of extra memory required per ray is thus proportional to $L \cdot (M+1)$ (at level $l = 0$, no stack is needed, though it is convenient to provide one).

Pseudo code for this algorithm is presented in Listing 2.

5 IMPLEMENTATION AND EVALUATION

Our approach relies on R*-trees (Beckmann et al., 1990) in 3D, and we only use triangles as geometric primitives for ray tracing static scenes. The numbers for minimum and maximum entries per node are set to $m = 2$ and $M = 4$, respectively, because this configuration yielded best results in our experiments. The R-trees are constructed on the CPU using pointers and are packed according to the proceeding described in Section 4 into a linear memory layout in a subsequent step. Rays are not packeted (Wald et al., 2001), but traced individually.

We implemented a simple CPU ray tracer designed for execution on common desktop computers using C++. The code relies in large parts on C++ templates, including some STL containers, and is mainly optimized by the compiler alone. The ray tracer merely allows basic parallel ray tracing by utilizing the compiler's OpenMP support in order to trace rays from C different rows of the resulting image concurrently, where C is number of CPU cores.

Our CUDA ray tracer accesses R-trees via a set of 1D textures. Positions of the first nodes $\Delta_L(l)$ at each

```
$t_{min} = \infty$;
stacks[$L+1$][$M$]; // entries at current level
distances[$L+1$]; // L + 1 is more convenient
sp[$L+1$]; // stack pointers
for ($n=0, l=L$; $n<N$; ) {
  if (! isEmptyNode($n$)) {
    if ($l>0$) { // visiting intermediate node
      sp[$l$] = 0;
      for ($i=0$; $i<M$; ++$i$) {
        $n' = n_e + i$;
        if (! isEmptyNode($n'$)) {
          $t$ = intersects(ray, getBox($n'$));
          if (($t<\infty$)$\wedge$($t<t_{min}$)) {
            stacks[$l$][sp[$l$]] = $n'$;
            distances[sp[$l$]] = $t$;
            ++sp[$l$];
          } }
      }
      sort(stack[$l$], distances, sp[$l$]);
    } else { // visiting leaf node
      foreach (triangle of $n$ as tri) {
        $t_{tri}$ = intersects(ray, tri);
        if (($t_{tri}<\infty$)$\wedge$($t_{tri}<t_{min}$))
          $t_{min}=t_{tri}$;
      }
      ++$l$; // done with this level
    } }
  while (($l \le L$)$\wedge$(sp[$l$] $<1$))
    ++$l$;
  if (($l \le L$)$\wedge$(sp[$l$] $>0$) {
    $n$ = stacks[$l$][--sp[$l$]];
    --$l$; // n is now from the next lower level
  } else
    $n=N$; // exit loop
}
return $t_{min}$;
```

Listing 2: Pseudo code for our algorithm for ordered ray traversal in R-trees. The algorithm requires additional memory to maintain a small stack per level (arrays stacks and sp). Function sort() performs in-place sorting of the stack according to the distances of the intersections from the ray's origin.

each level l are precomputed and stored together with the number of an R-tree's maximum level L in the constant memory area of the ray tracer's kernel. In all cases, we achieved best performance results when running CUDA ray tracing kernels in a configuration of h blocks with 128 threads each, where h is the number of rows in the rendered image.

All measurements in the following were obtained on a desktop computer with an Intel i7-4820K CPU at 3.7 GHz, 32 GB RAM and an NVIDIA GeForce GTX 780 graphics adapter with 3 GB memory (NVIDIA Corp., 2014). Images were rendered at resolutions of 1024×1024 pixels, so that $h = 1024$ for all CUDA kernel executions. The CPU ray tracer was executed using all $C = 8$ processor cores available.

SCITEPRESS SCIENCE AND TECHNOLOGY PUBLICATIONS

5.1 Comparison of R-Tree Construction Schemes

We constructed R*-trees by successive insertion of triangles and investigated the following strategies for selecting nodes (cf. Section 2.2.1):

1. `minVolume`: minimize the volume enlargement of nodes, regardless of their level. This is the same strategy employed by the original R-tree (Guttman, 1984).
2. `minSurface`: minimize the surface area enlargement of nodes. This corresponds to the surface area heuristic (SAH) (MacDonald and Booth, 1990).
3. `minOverlap`: minimize the mutual overlap of nodes, resolve ties by selecting the node that needs least volume enlargement
4. `R*-tree`: minimize the volume enlargement at intermediate nodes and the overlap at leaf nodes
5. `R*-treeSrfc`: similar to `R*-tree`, but minimize the surface enlargement at intermediate nodes and the overlap at leaf nodes

Alterations of the method for splitting nodes presented in (Beckmann et al., 1990), like using volume as measurements for determining split axes or redistributing entries, only impaired ray tracing performance, and we thus relied on the original approach. The influence of the node selection strategies on ray tracing performance is summarized in Table 1. The values were obtained by rendering our test scenes from the fixed camera poses shown in Figure 1 using primary and shadow rays. For ray traversal by means of our CPU implementation, we employed the stackless algorithm presented in Section 4.1, whereas our GPU tracer relied on the method for ordered traversal described in Section 4.2.

The results in Table 1 show that the two strategies based on minimizing surfaces of AABBs, i.e., `R*-treeSrfc` and `minSurface`, are best for constructing R*-trees for the purpose of ray tracing. Minimizing the mutual overlap by means of `minOverlap` diminished the performance considerably, especially in case of the `Bunny` test scene where CPU ray tracing performance was degraded by $\approx 2690\%$ and our CUDA ray tracer even failed to launch.

Furthermore, the results indicate a correlation between the insertion strategy and the geometry of a scene and can be explained as follows:
Strategy `minSurface` favors the formation of boxes of cubic shape, whereas `minVolume` prefers flat boxes that may have zero extension along one axis and thus zero volume, but which may have large surfaces. Both strategies can reduce dead space, but `minSurface` outperforms `minVolume` for the same reason that makes SAH the preferred method for building kd-trees: Provided the origins and directions of rays are uniformly distributed in space, the conditional probability of a ray intersecting a box B_1 to intersect a completely contained box B_2 is approximately proportional to the ratio $\frac{\mathcal{S}(B_2)}{\mathcal{S}(B_1)}$ of their *surfaces* $\mathcal{S}(B_i), i \in \{1,2\}$ (see (MacDonald and Booth, 1990; Wald and Havran, 2006)). Strategy `minSurface` chooses the node where this probability is highest, and the intersection test between a ray and the outer box is thus less likely to be redundant.

Table 1: The strategies for selecting nodes where triangles are inserted into R-trees directly influence their structure and thus their performance in ray tracing. Values were obtained by tracing primary and shadow rays. Using `minOverlap` and the `Bunny` test scene, our CUDA kernels failed to launch and we were unable to obtain results.

	scene	minVolume	minSurface	minOverlap	R*-tree	R*-treeSrfc
CPU	Bunny	1.95 s	1.59 s	53.0 s	1.90 s	1.57 s
	Cath.	6.40 s	4.95 s	13.6 s	5.39 s	3.54 s
	Fairy	5.92 s	3.31 s	8.50 s	5.65 s	3.41 s
	Conf.	3.99 s	3.30 s	5.79 s	3.94 s	3.01 s
GPU	Bunny	67 ms	63 ms	–	71 ms	59 ms
	Cath.	221 ms	162 ms	478 ms	201 ms	138 ms
	Fairy	169 ms	98 ms	263 ms	158 ms	104 ms
	Conf.	134 ms	113 ms	199 ms	134 ms	98 ms

Strategy `minOverlap` assigns entries to nodes regardless of dead space. This behavior is particularly problematic at upper R-tree levels, where AABBs occupy potentially large volumes that may have to overlap due to the scene geometry. In case of the `Bunny` scene, the virtual camera is moreover not located as deep "inside" the R-tree as in the other scenes, but is surrounded by only few AABBs from levels close to L. Hence, much more tests for intersection with rays and AABBs of large volume are needed, which explains the poor performance of this method.

The strategies `R*-tree` and `R*-treeSrfc` are composed of `minOverlap` and `minVolume` or `minSurface`, respectively. However, only leaf nodes are subject to `minOverlap`, and triangles are "directed" already towards their respective parents based on spatial locality and on (local) minimization of dead space at higher levels. Optimizing for mutual overlap of leaf nodes results in a reduction of the number of paths that need to be followed during traversal in R-trees. In this way, better performances are yielded than in cases of `minVolume` and `minSurface`. This proceeding has been reported to be a means

SCITEPRESS SCIENCE AND TECHNOLOGY PUBLICATIONS

Table 2: Ray tracing performance of R-trees when omitting forced reinserts during construction by means of R*-treeSrfc strategy.

	Bunny	Cathedral	Fairy	Conference
CPU	1.92 s	4.42 s	3.81 s	3.01 s
	(−23%)	(−25%)	(−12%)	(±0%)
GPU	69 ms	154 ms	115 ms	105 ms
	(−17%)	(−12%)	(−11%)	(−7%)

of improving the performance of R*-trees over R-trees (Beckmann et al., 1990) and is confirmed by our results.

In addition, we found that forced reinserts used with R*-trees improve their structure and ray tracing performance in most cases. The results we obtained when sparing forced reinserts during construction of R-trees by means R*-treeSrfc strategy are given in Table 2.

5.2 Comparison of Ray Traversal Algorithms

We evaluated the two algorithms for tracing rays in R-trees presented in Section 4 by means of our CPU and GPU ray tracer, respectively. Performance was measured in the same way as described in Section 5.1 with R-trees being constructed using the R*-treeSrfc strategy and forced reinserts. In case of ordered ray traversal, the auxiliary stacks were sorted using insertion sort, because this sorting algorithm is easy to implement, in-place and efficient for small data sets (Sedgewick, 2002). We also acquired timings by using a conventional stack-based traversal algorithm in our CPU implementation for comparison. The results are given in Table 3.

Table 3: Ray tracing performances of R-trees using the traversal algorithms presented in Section 4 and a common stack-based method (CPU ray tracer only).

	scene	stackless	ordered	stack
CPU	Bunny	1.57 s	1.82 s	2.09 s
	Cathedral	3.54 s	4.23 s	5.94 s
	Fairy	3.41 s	3.77 s	4.41 s
	Conference	3.01 s	3.37 s	3.81 s
GPU	Bunny	65 ms	59 ms	–
	Cathedral	120 ms	138 ms	–
	Fairy	102 ms	104 ms	–
	Conference	98 ms	98 ms	–

In most cases, best performance was achieved by means of the stackless algorithm for ray traversal. The ordered algorithm proved to be somewhat better in case of the Bunny scene, in which the virtual camera was placed at a location contained only by few AABBs at higher levels of the R-tree. In the remaining scenes, the camera was located deeper inside the R-trees. Hence, sorting nodes based on their distances from the origins of the rays was needles in most situations, and the accompanying overhead diminished the ray tracing performance. However, if we placed the virtual camera outside the AABBs of R-trees, our ordered ray traversal outperformed the stackless method. For instance, rendering the Cathedral scene by means of our GPU ray tracer from a virtual viewpoint outside the R-tree took 51 ms using the ordered traversal method, compared to 68 ms using the stackless algorithm. We therefore propose to employ the presented traversal algorithms for R-trees with respect to the position of the virtual camera.

5.3 Comparison with KD-Trees

We compared the performance of R-trees in our CPU ray tracer to timings we obtained from ray tracing by means of kd-trees. The kd-trees were constructed using the local greedy surface area heuristic (SAH) and the $O\left(n\log^2(n)\right)$ algorithm described in (Wald and Havran, 2006). The method we employed to traverse kd-trees is the stack-based algorithm given in (Hapala and Havran, 2011). For the sake of better comparability, we compare kd-tree traversal to a more similar stack-based algorithm for traversing R-trees. The R-trees were again constructed using R*-treeSrfc strategy and forced reinserts. Both traversal algorithms are merely optimized to the effect that they skip AABBs/half spaces which are further away from a ray's origin than any intersection with a triangle already encountered. The results are listed in Table 4 and were obtained by rendering our test scenes twice from the fixed camera poses shown in Figure 1: one time by tracing primary rays only, and another time using primary and shadow rays.

With the exception of the Bunny scene, the perfor-

Table 4: Timings in seconds from our comparison of R-trees and kd-trees for ray tracing. Kd-trees were traversed using a stack-based algorithm, and the results given for R-trees apply to the stack-based traversal scheme also employed in Section 5.2. The corresponding results for primary and shadow rays are hence identical to those given in Table 3.

	scene	R*-tree	kd-tree
primary rays	Bunny	1.38 s	1.59 s
	Cathedral	3.30 s	2.04 s
	Fairy	2.59 s	2.23 s
	Conference	2.43 s	2.14 s
primary and shadow rays	Bunny	2.09 s	2.96 s
	Cathedral	5.94 s	4.01 s
	Fairy	4.41 s	3.96 s
	Conference	3.81 s	3.46 s

mance of kd-trees for ray tracing was superior to those of R-trees. In case of Bunny, the better performance of R-trees results from the small number of triangles in that scene instead of from the position of the virtual camera. In similar scenes consisting of less than ≈ 100000 triangles, but not presented in this work, we found ray tracing by means of R-trees always to be faster.

If we compared the results of stackless R-tree traversal on CPUs in Table 3 to the corresponding timings of stack-based kd-tree traversal in Table 4, ray tracing using R-trees would be the faster method. Since we did not consider alternatives for stackless kd-tree traversal, we deem such a comparison between two fundamentally different algorithms and any conclusions drawn from it inappropriate.

5.4 Construction Times

Although this work is not focused on the times needed for constructing R*-trees, it is worth mentioning that they are significantly lower than the times required for constructing SAH kd-trees by means of the $O(n \log^2(n))$ algorithm presented in (Wald and Havran, 2006). We list the times from our implementation in Table 5 primarily to provide indications for other researchers and potential future work.

Table 5: Timings in seconds required for constructing spatial indexes containing our test scenes shown in Figure 1. R-trees were constructed using forced reinserts.

scene	R*-tree	kd-tree
Bunny	0.61 s	7.03 s
Cathedral	0.62 s	4.37 s
Fairy	1.63 s	20.02 s
Conference	2.91 s	27.59 s

In case of our test scenes Bunny and Conference, the timings we obtained for kd-trees are remarkably similar to those reported in (Wald and Havran, 2006) (6.7 s and 30.5 s, respectively), although we have different hardware and an independent implementation. The build times of the $O(n \log(n))$ algorithm the authors presented in that work (3.2 s and 15.0 s, respectively), are also much higher than the times required for building R*-trees. The latter in turn, are yet significantly higher than the times for building BVHs of scenes corresponding to Bunny and Conference by the sophisticated methods presented in (Wald, 2007).

6 CONCLUSIONS AND FUTURE WORK

In this article, we gave a first demonstration of the suitability of R-trees for accelerating ray tracing. We presented two algorithms for traversing R-trees that exploit the regularity of these data structures in order to compute intersections between the geometric primitives stored within and rays. The method for stackless traversal requires neither to restructure the trees nor extra memory for internal pointers or other. Although our algorithm for ordered traversal may perform better with certain camera poses, the stackless variant is particularly interesting due to its simplicity and suitability for implementation on modern GPUs. Ray traversal on GPUs might be further improved by exploiting the fixed path lengths of R-trees and careful optimization. In addition, we have only traced individual rays and neglected the influence of ray coherence so far, but packeting rays as presented in (Wald et al., 2001; Günther et al., 2007) is likely to increase ray tracing performance of R-trees.

Moreover, we investigated construction schemes for R-trees and their influence on ray tracing performance. We showed that altering the measure from volume to surface in the original strategy of R*-trees for selecting nodes for data insertion results in a considerable improvement. More sophisticated methods for constructing R-trees, like the ones used with RR*-trees (Beckmann and Seeger, 2009), for example, or bulk-loading data (Sellis et al., 1987; Arge et al., 2008) might yield even better results. These methods could probably benefit from ideas designed for optimizing BVHs, such as the ones presented in (Wächter and Keller, 2006; Wald, 2007).
Our direct comparison with kd-trees showed that these yield better performance results in most situations yet, but the employment of stackless methods for R-tree traversal appears preferable over stack-based kd-tree traversal.

Major points for optimizing the performance of R-trees in ray tracing might also be revealed by thoroughly investigations of the caching behavior of R-trees on GPUs.

Considering the simplicity of ray traversal and the potentially high data locality that result from their regular structure, R-trees may become a competitive choice for accelerating GPU ray tracing as more research is done on this subject.

ACKNOWLEDGMENTS

We thank all persons who created the models we used throughout this work and made them publicly available. Additionally, we give thanks to M. Pohl for her helpful comments on this article.

REFERENCES

Arge, L., Berg, M. D., Haverkort, H., and Yi, K. (2008). The Priority R-tree: A Practically Efficient and Worst-case Optimal R-tree. *ACM Trans. Algorithms*, 4(1):9:1–9:30.

Bayer, R. and McCreight, E. (1972). Organization and Maintenance of Large Ordered Indexes. *Acta Informatica*, 1(3):173 – 189.

Beckmann, N., Kriegel, H.-P., Schneider, R., and Seeger, B. (1990). The R*-tree: An Efficient and Robust Access Method for Points and Rectangles. In *SIGMOD '90: Proceedings of the ACM SIGMOD International Conference on Management of Data*, volume 19(2), pages 322–331. ACM.

Beckmann, N. and Seeger, B. (2009). A Revised R*-tree in Comparison with Related Index Structures. In *Proceedings of the 2009 ACM SIGMOD International Conference on Management of Data*, SIGMOD '09, pages 799–812. ACM.

Günther, J., Popov, S., Seidel, H.-P., and Slusallek, P. (2007). Realtime Ray Tracing on GPU with BVH-based Packet Traversal.

Guttman, A. (1984). R-trees: A Dynamic Index Structure for Spatial Searching. In *SIGMOD '84: Proceedings of the ACM SIGMOD International Conference on Management of Data*, pages 47–57. ACM.

Hachisuka, T. (2009). Ray Tracing on Graphics Hardware. Technical report, University of California at San Diego.

Hapala, M., Davidovič, T., Wald, I., Havran, V., and Slusallek, P. (2011). Efficient Stack-less BVH Traversal for Ray Tracing. In *Proceedings of the 27th Spring Conference on Computer Graphics*, SCCG '11, pages 7–12, New York, NY, USA. ACM.

Hapala, M. and Havran, V. (2011). Review: Kd-tree Traversal Algorithms for Ray Tracing. *Computer Graphics Forum*, 30(1):199–213.

Horn, D. R., Sugerman, J., Houston, M., and Hanrahan, P. (2007). Interactive K-d Tree GPU Raytracing. In *Proceedings of the 2007 Symposium on Interactive 3D Graphics and Games*, I3D '07, pages 167–174, New York, NY, USA. ACM.

MacDonald, D. J. and Booth, K. S. (1990). Heuristics for Ray Tracing Using Space Subdivision. *The Visual Computer*, 6(3):153–166.

NVIDIA Corp. (2014). GeForce GTX 780 Specifications. http://www.geforce.com/hardware/desktop-gpus/geforce-gtx-780/specifications.

Oracle Corp. (2014a). MySQL 5.6 Reference Manual. http://downloads.mysql.com/docs/refman-5.6-en.a4.pdf.

Oracle Corp. (2014b). Oracle Spatial and Graph Developer's Guide. http://docs.oracle.com/database/121/SPATL/E49172-03.pdf.

Samet, H. (2006). *Foundations of Multidimensional and Metric Data Structures*. Morgan Kaufmann, 1st edition.

Sedgewick, R. (2002). *Algorithms in Java Parts I – IV*. Addison Wesley, 3rd edition.

Sellis, T. K., Roussopoulos, N., and Faloutsos, C. (1987). The R+-Tree: A Dynamic Index for Multi-Dimensional Objects. In *Proceedings of the 13th International Conference on Very Large Data Bases*, VLDB '87, pages 507–518, San Francisco, CA, USA. Morgan Kaufmann Publishers Inc.

Stich, M., Friedrich, H., and Dietrich, A. (2009). Spatial Splits in Bounding Volume Hierarchies. In *Proceedings of the Conference on High Performance Graphics 2009*, HPG '09, pages 7–13, New York, NY, USA. ACM.

Suffern, K. (2007). *Ray Tracing from the Ground Up*. A. K. Peters, Ltd., 1st edition.

Sylvan, S. (2010). R-trees: Adapting Out-Of-Core Techniques to Modern Memory Architectures. Talk at Game Developers Conference, http://gdcvault.com/play/1012452/R-Trees-Adapting-out-of.

Wächter, C. and Keller, A. (2006). Instant Ray Tracing: The Bounding Interval Hierarchy. In *Proceedings of the 17th Eurographics Conference on Rendering Techniques*, EGSR'06, pages 139–149, Aire-la-Ville, Switzerland, Switzerland. Eurographics Association.

Wald, I. (2007). On Fast Construction of SAH-based Bounding Volume Hierarchies. In *Proceedings of the 2007 IEEE Symposium on Interactive Ray Tracing*, RT '07, pages 33–40, Washington, DC, USA. IEEE Computer Society.

Wald, I. and Havran, V. (2006). On Building Fast kd-Trees for Ray Tracing, and on Doing That in O(N log N). In *Proceedings of the 2006 IEEE Symposium on Interactive Ray Tracing*, pages 61–70.

Wald, I., Mark, W. R., Günther, J., Boulos, S., Ize, T., Hunt, W., Parker, S. G., and Shirley, P. (2007). State of the Art in Ray Tracing Animated Scenes. In *STAR Proceedings of Eurographics 2007*, pages 89–116. The Eurographics Association.

Wald, I., Slusallek, P., Benthin, C., and Wagner, M. (2001). Interactive Rendering with Coherent Ray Tracing. In *Computer Graphics Forum*, pages 153–164.

Zlatuska, M. and Havran, V. (2010). Ray Tracing on a GPU with CUDA – Comparative Study of Three Algorithms. In *Proceedings of WSCG'2010, communication papers*, pages 69–76.